2008

# An Observational Analysis and Evaluation of Land Surface Model Accuracy in the Nebraska Sand Hills

David B. Radell
*University of Nebraska-Lincoln*, dave@bigred.unl.edu

Clinton M. Rowe
*University of Nebraska-Lincoln*, crowe1@unl.edu

# An Observational Analysis and Evaluation of Land Surface Model Accuracy in the Nebraska Sand Hills

DAVID B. RADELL AND CLINTON M. ROWE

*Department of Geosciences, University of Nebraska—Lincoln, Lincoln, Nebraska*

(Manuscript received 30 March 2007, in final form 24 September 2007)

ABSTRACT

In this study, the influence of subsurface water on the energy budget components of three locations with heterogeneous land surfaces in the Nebraska Sand Hills are examined through observations and use of the Noah land surface model (LSM). Observations of the four primary components of the surface energy budget are compared for a wet interdunal meadow valley, a dry interdunal valley, and a dunal upland location. With similar atmospheric forcing at each site, it was determined that differences in the partitioning of the mean diurnal net radiation ($R_{net}$) existed among the three locations due to the influence of varied soil moisture and vegetation through the year. At the wet valley, observations indicated that almost 65% of the mean daily peak $R_{net}$ was used for latent heating, due to the relatively higher soil moisture content resulting from an annual upward gradient of subsurface water and denser vegetation. In sharp contrast, the dunal upland site yielded only 21% of the mean daily peak $R_{net}$ going to latent heating, and a greater mean diurnal soil heat flux with typically drier soils and sparser vegetation than at the wet valley. The dry valley partition of the peak $R_{net}$ fell between the wet valley and dunal upland site, with approximately 50% going to sensible heating and 50% toward latent heating. In addition to the observational analysis, an uncoupled land surface model was forced with the observations from each site to simulate the energy budgets, with no tuning of the model's fundamental equations and with little adjustment of the model parameters to improve results. While the model was able to reasonably simulate the mean diurnal and annual energy budget components at all locations, in most instances with root-mean-square errors within 20%–25% of the observed values, the lack of explicit treatment of subsurface water within the model limited predictability, particularly at the wet valley site. For instance, only 25% of the peak mean diurnal $R_{net}$ went toward latent heating in the model simulation of the wet valley, compared to 65% as estimated by observations. Model evaluation statistics are presented to document the land surface model's ability to capture the annual and mean diurnal variations in the surface energy budget terms at the dry valley and dunal upland sites, but the absence of subsurface water results in large errors in the wet valley simulation. From these results, a case is made for the future inclusion of the explicit treatment of subsurface water within the Noah LSM to better approximate the prediction of the surface energy budget in such environments.

## 1. Introduction

The Nebraska Sand Hills (Fig. 1) are a unique part of the Missouri River basin that can be expected to exert an influence on local and regional atmospheric conditions due to their large size and physiographic characteristics, including a vast accumulation of subsurface water as part of the High Plains Aquifer. The Sand Hills are characterized by approximately 50 000 km$^2$ of rolling sand sheets and dunes, with typical elevations of 1 km above sea level and local relief of the highest dunes near 0.1 km (Bleed and Flowerday 1998). Climatically, the Nebraska Sand Hills are situated in a semiarid region, averaging nearly 500 mm yr$^{-1}$ of precipitation, much of which occurs during the warm season. Most of the region is covered with short rangeland grass and shrub vegetation, although interdune wetland areas consisting of denser mixtures of short prairie grasses occupy an estimated 4000 km$^2$ (Gosselin et al. 2006). The interdune regions are unique, in that the water table depth can vary significantly with the seasons (Chen and Hu 2004). The water table is close to or often above the land surface, providing plentiful moisture for the soils and vegetation in the interdunal regions. The soils that compose the Sand Hills and sur-

*Corresponding author address:* David B. Radell, Department of Geosciences, University of Nebraska—Lincoln, 214 Bessey Hall, Lincoln, NE 68588-0340.
E-mail: dave@bigred.unl.edu

DOI: 10.1175/2007JHM913.1

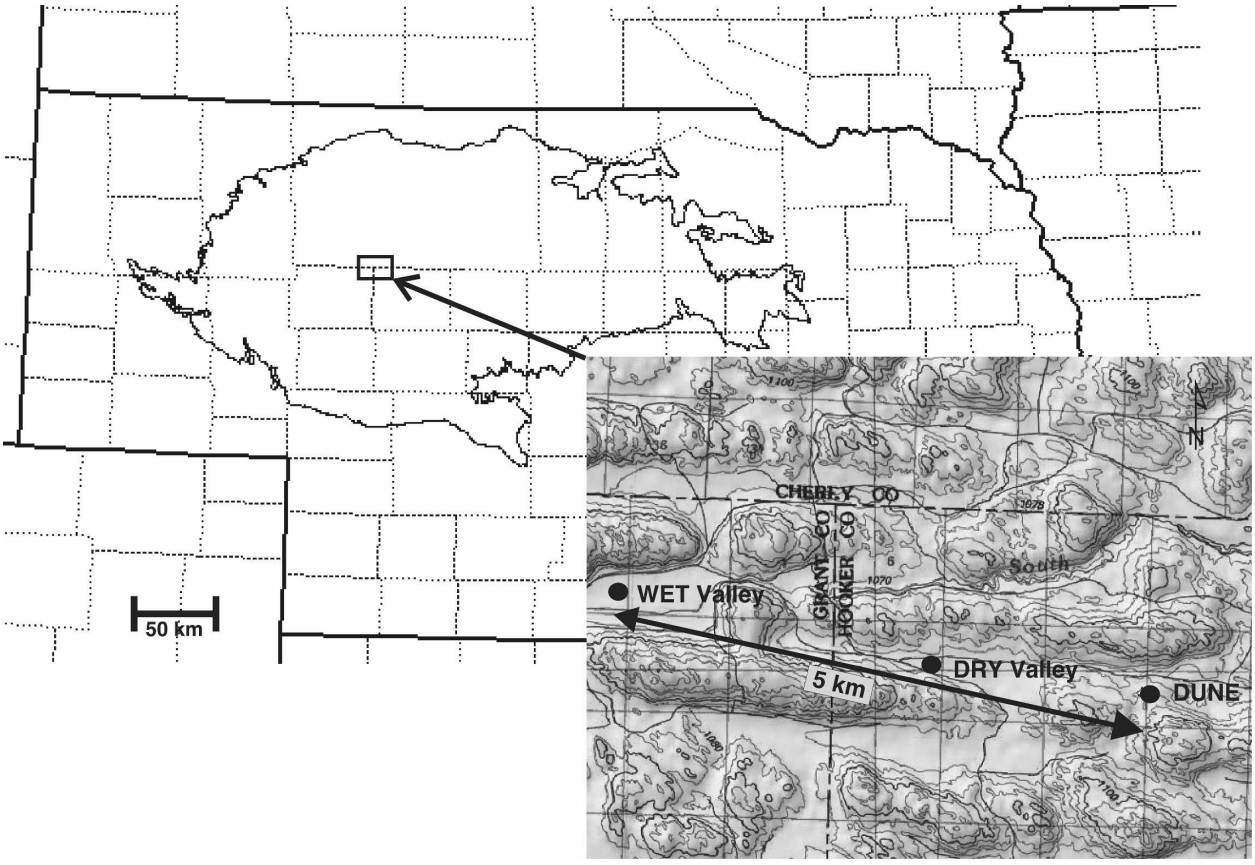


FIG. 1. Location of the Sand Hills and the meteorological observing sites used in the study. The location of the Sand Hills is outlined in solid black. Contour intervals in the inset are 25 m.

rounding regions are chiefly eolian dune sand, as well as combinations of silt, clay, gravel, and peat in the interdune regions. The large dunes that compose the Sand Hills were formed chiefly by drifting sand that accumulated here in the last 8000 yr, and are now held in place by the prairie grasses that dominate (Bleed and Flowerday 1998).

The physical soil properties of the Sand Hills allow for a large percentage of incident precipitation to quickly infiltrate the sandy dunes and accumulate as groundwater over geologically short time scales. The High Plains Aquifer is recharged from the accumulated subsurface water, and provides much of the available root zone soil moisture to the interdunal valleys of the region, as a net upward gradient in soil water exists in the wettest valleys (Gosselin et al. 1999; Chen and Hu 2004). Thus, due to the influence of this accumulated water, evapotranspiration (ET) exceeds precipitation throughout most of the year, particularly in the interdune valleys of this semiarid region.

Land surface–atmosphere interactions in semiarid environments such as the Sand Hills have been examined in depth (Findell and Eltahir 1997; Small and Kurc 2003; Hogue et al. 2005). To our knowledge, however, there has been little research focused on an environment where subsurface water influences the soil moisture and energy budget to such an extent, with observing stations in close proximity. The major goals of this research are the following:

1) To document and compare the observed differences in energy and water exchanges between the surface and atmosphere over diurnal and annual time scales for three distinct landscapes: one with a significant contribution from subsurface water, one with varied contribution, and one with no subsurface water influence.
2) To test the ability of a commonly used land surface model to capture the exchanges of energy and water between the surface and atmosphere and to evaluate its accuracy in an environment where atmospheric forcing is similar yet the land surface is heterogeneous.

Data from three energy balance–Bowen ratio (EBBR) micrometeorological towers were used to assess the relative contributions of the energy budget components

for each site over a 1-yr period. Atmospheric data for 2004 from a wet meadow interdunal valley (WET), a dry interdunal valley (DRY), and a dunal upland (DUNE) location (Fig. 1) were analyzed to assess the impact of the different vegetation and soils over a variety of temporal scales (e.g., daily to annual). These locations were chosen to represent the predominant land surfaces found within the region and for their proximity to one another to minimize differences in atmospheric forcing.

The meteorological data at each site were used as atmospheric forcing to drive the National Centers for Environmental Prediction–Oregon State University–Air Force Weather Agency–Hydrologic Research Laboratory (Noah) land surface model (LSM; Mahrt and Pan 1984; Chen et al. 1996; Chen and Dudhia 2001a; Ek et al. 2003), to test its ability to simulate surface exchanges of energy and water. The Noah LSM is a robust, multilayer soil and vegetation model currently coupled to many numerical weather prediction (NWP) models, such as the operational North American Mesoscale (NAM) model, the research-oriented fifth-generation Pennsylvania State University–National Center for Atmospheric Research (PSU–NCAR) Mesoscale Model (MM5; Chen and Dudhia 2001b) and, more recently, the Weather Research and Forecasting (WRF) Model (Skamarock et al. 2005). The Noah LSM was chosen for this study due to its robustness and success in regions of semiarid climate similar to that of the Sand Hills, such as the Konza Prairie in Kansas (Chen et al. 1996; Evans et al. 2005) and the upper San Pedro River basin in southeastern Arizona (Hogue et al. 2005). To assess the model's predictive success, evaluation was performed against observed and derived components of the surface energy and water budgets from the three EBBR meteorological towers. Section 2 describes the characteristics of each site and analyzes and compares the mean diurnal characteristics of the locations. Section 3 describes the Noah LSM and experimental design employed in this study, and section 4 presents an analysis and discussion of the model simulations. Section 5 offers conclusions and a summary of the major findings.

## 2. Atmospheric forcing data and methodology

### *a. Site descriptions*

The three meteorological observing sites used in this study are located near Gudmundsen, Nebraska, in the northwestern region of the state (Fig. 1) at the University of Nebraska's Gudmundsen Sand Hills Research Laboratory (GSL). The meteorological sites are geographically close (Fig. 1), with the WET site located approximately 5 km to the west-northwest of the DUNE site and 3 km west-northwest of the DRY site. The WET site is located at an elevation of approximately 1060 m above mean sea level (MSL), in a valley of about 8 km in length (Gosselin et al. 1999), with dunes 25–70 m high surrounding the valley (Fig. 1, inset). There is a small drainage ditch located about 0.5 km south of the observing platform in the wet meadow, which acts to drain the valley during times of high water levels, particularly during the early spring (Gosselin et al. 2006). The water table is high here throughout the year, and plays a pivotal role in the root zone soil moisture profile. According to Gosselin et al. (1999), piezometer measurements taken over a 2.5-yr period at four locations within the wet valley show that a net upward vertical gradient of subsurface water exists here throughout the year. They further document a large reservoir of groundwater located just to the north of the WET valley floor, which serves to supply the wet valley with plentiful soil water as flow is directed into the valley. Due to the increased subsurface water component, the vegetation is largely homogenous and relatively lush within this valley, with heights of approximately 0.15 m, and consisting mainly of C3 and C4 grasses, alfalfa, and small cactus (Gosselin et al. 1999). The soils here are predominately sand, though peat and finer clay material have been noted in valley regions as well (Bleed and Flowerday 1998).

The DRY site also resides in a flat interdune valley with an elevation of 1060 m MSL, and is surrounded by dunes of 25–40 m high on all sides except to the east (Fig. 1, inset). While this valley is considered to be "dry," it is so only as compared to the WET valley, as vegetation does exist but tends to be more heterogeneous and have smaller fractional coverage (Gosselin et al. 1999). Soil composition is similar to the WET valley. The valley floor is generally dry (Gosselin et al. 2006), indicating that the water table is below the surface for much of the year, and there exists a predominately downward vertical gradient of subsurface water (Gosselin et al. 1999).

The DUNE site is located at an elevation of 1080 m (or 20 m higher than the valley locations). It is characterized by sparse prairie grass, and the area soils are predominately pure sand, with little or no clay or peat material present and a water table far below the surface having negligible influence on the root zone soil moisture content.

### *b. Observed data*

The basic assumption of EBBR theory is that the sum of the net radiation and soil ($G$), sensible ($H$), and latent heat (LE) fluxes at the surface must be zero,

which assumes that the net radiation is distributed only among those three components and the energy budget is balanced. The energy budget at the earth's surface is therefore

$$R_{\text{net}} - H - \text{LE} - G = 0. \quad (1)$$

The EBBR observing towers at each of the Sand Hills' locations collected observations of numerous atmospheric variables at two levels (2.1 and 3.6 m) every 2 s. Half-hourly averages of air temperature, relative humidity, station pressure, wind speed and direction, downwelling shortwave radiation, and net radiation were measured and stored. The soil heat flux was estimated by two plates (Radiation and Energy Balance Systems HFT-3) located at 0.05 m below the ground surface and a mean value was taken. No attempt was made to account for heat stored in the soil above them, but it should be noted that a correction factor of approximately 15–40 W $m^{-2}$ would account for the difference between ground heat flux measured at depth (0.1 m) and the surface (as in the Noah model). Soil moisture was measured at the DRY and DUNE sites, at depths of 0.10, 0.25, 0.50, and 1 m (0.8 m at the dry valley) and soil temperature at 0.1 m was also recorded. No soil moisture data were available for the wet valley. At each site, a tipping-bucket rain gauge recorded liquid precipitation with a sensitivity of 0.1 mm per tip, and the data recorded represented the cumulative number of tips over a 30-min period. From the each of the variables described above, numerous additional meteorological variables were derived over both 30-min periods and for 24-h periods. These included saturation vapor pressure at 2.1 and 3.6 m, latent and sensible heat flux estimates, potential and actual evapotranspiration, and daily high and low temperatures.

The raw recorded and derived data were then quality controlled for accuracy. This included omitting data that were the result of a broken or bad sensor (for derived quantities), data that were simply missing, or data that were out of range of reasonable values (the range limits depended upon the variable but were consistent among the three locations). Soil moisture was omitted during times when the soil temperature sensor reported values less than 273 K because of manufacturer limitations. In addition, a well-known limitation of the EBBR method of estimating surface fluxes are the sometimes unrealistic values encountered when respective temperature and moisture gradients are small, such as during dawn, dusk, or overnight hours (Stull 1988). Many flux observations that fell outside the predetermined bounds were removed before the model evaluation. In some cases, even though the energy budget was technically "balanced," the latent heat flux still retained unrealistically large, negative values. To account for these cases, a minimum value of $-20$ W $m^{-2}$ (which corresponds to 0.03 mm $h^{-1}$ of dewfall) was set as a lower boundary for the latent heat flux, and all energy budget component data were omitted if this threshold was exceeded. Monteith (1963) reports that a maximum dewfall rate of 0.067 mm $h^{-1}$ can occur on vegetation under saturated conditions over a wide temperature range with light winds, and can be thought of as an "upper limit" of dewfall. Furthermore, this "potential" condensation rate may be overestimated by 10%–20% because of the assumption that the vegetation is a blackbody (Monteith 1963). Therefore, a threshold of 0.03 mm $h^{-1}$, roughly half of the theoretical potential rate, was used because of the arid Sand Hills environment. The resulting quality control methods ensured that only the best data were used for analysis. Even with these strict boundaries, several thousand observations were used (without the need to average over longer time periods) in the analysis to evaluate the land surface model. Most missing observations were confined to the DRY site, where many cool season days and overnight observations were unavailable, resulting in only about one-half the number of total observations relative to the WET and DUNE sites. In many instances at all three sites, the observations nearest to sunrise and sunset were omitted because of large vertical gradients in temperature and moisture resulting in unrealistic Bowen ratio values.

### c. *Analysis of the observed annual cycle*

Numerous authors have documented the effect on the atmosphere resulting from the forcing by the land surface over many scales (e.g., McCumber and Pielke 1981; Anthes 1984; Twine et al. 2004). Soil moisture is crucial to the land surface–atmosphere system, controlling the partitioning of the surface energy budget and contributing to the water cycle via evapotranspirative processes (Mahmood and Hubbard 2004). In addition, soil moisture controls the partition of sensible and latent heat and influences the near-surface meteorology (Small and Kurc 2003; Juang et al. 2007). The importance of accurate representation of soil moisture in land surface models has been well documented (Mohr et al. 2000; Ronda et al. 2002) with respect to increasing the accuracy of surface flux estimates. However, the representation of subsurface water and its influence on soil moisture, particularly over small spatial and temporal scales, has received less attention. Maxwell and Miller (2005) report that by adding a coupled groundwater model to a single-column land surface model, an improvement in the prediction of the root zone soil moisture profile is noted. Moreover, Chen and Hu (2004)

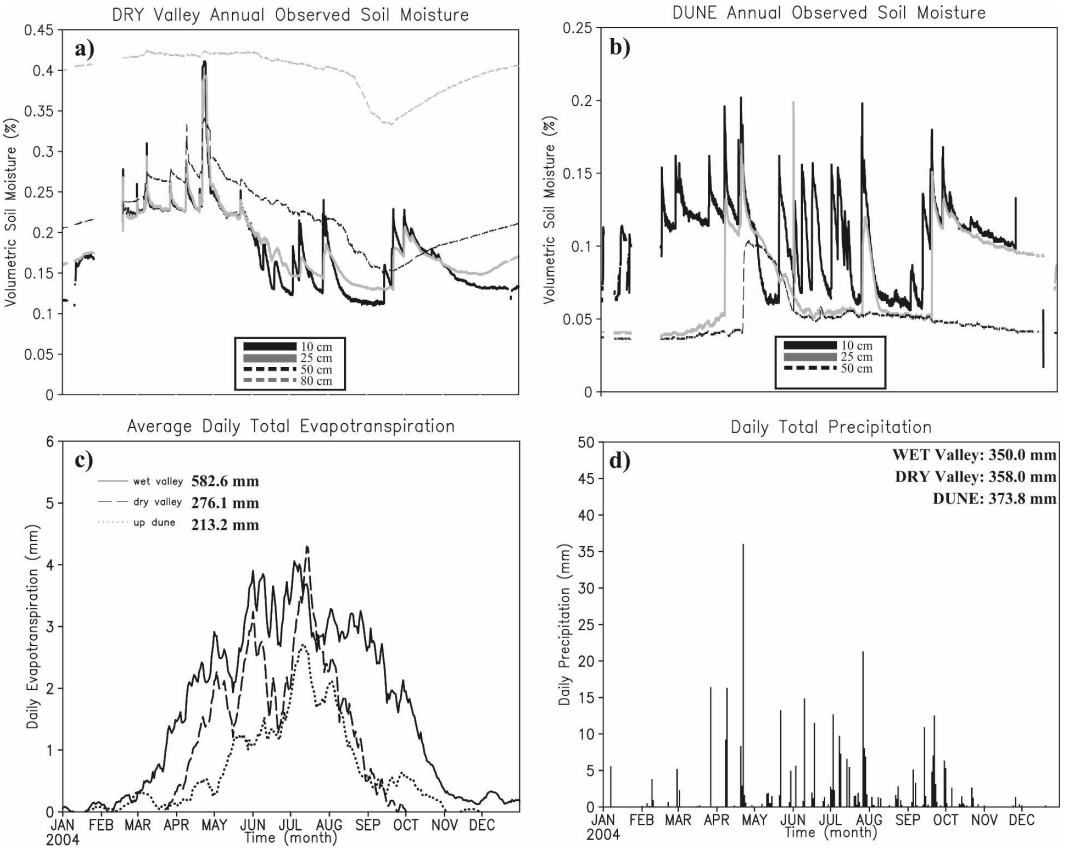


FIG. 2. (a) DRY valley volumetric soil moisture and (b) DUNE volumetric soil moisture. Note that only the 10-, 25-, and 50-cm depths are presented for this site. (c) The Bowen ratio (Allen et al. 1998) average daily total evapotranspiration (mm) for the three Sand Hills locations. Cumulative annual evapotranspiration (mm) estimates for each observing station are given in the legend. (d) The daily precipitation (2004) averaged over the three sites with cumulative totals for each site given in the legend.

state that surface evaporation was closer to the observed values, increasing by 7%–21%, and that the area-averaged evaporation over a 72 km$^2$ area in the Sand Hills almost doubled when a source of subsurface water was included. It is therefore expected that the ET at the WET and DRY locations are in part controlled by the variations in depth to groundwater, particularly over the warm season when potential evapotranspiration (PET) is high and soil moisture is low, which is not currently treated explicitly in the Noah model.

At two of the three Sand Hills locations, soil water observations were available at four depths (10, 25, 50, and either 80 or 100 cm) during the 2004 annual cycle (Figs. 2a,b). Observations were not available at the WET site due to the frequently saturated soil at the surface there and for the lowest soil depth (100 cm) at the DUNE location. The DRY site, with a higher percentage of clay and organic matter than the DUNE location (Bleed and Flowerday 1998), has a greater capacity to store soil water throughout the root zone (Fig. 2a). At the 25- and 50-cm levels of the DRY and DUNE locations (Figs. 2a,b), the soil moisture differed between the sites. A noticeable drop in the root zone begins at each location by early May, as precipitation decreases and ET becomes a depleting influence on the local soil moisture until September. It is at this time that the soil moisture approaches the wilting point at the DUNE location (Fig. 2b), but begins to increase at the DRY site through the remainder of the year particularly at the lowest levels (Fig. 2a). This suggests that an outside source contributes to increasing the soil moisture here past the growing season, especially after mid-October, and into December. Noticeable variation existed at the 10-cm depth, with quick response to precipitation events displayed at both locations. At the DUNE site (Fig. 2b), where coarse sandy soils allow for faster infiltration and lower retention of precipitation in the upper soil layers, soil moisture is less than at the DRY site at all depths throughout the year.

Annual trends in soil moisture content at these Sand Hills' locations (Figs. 2a,b) are related to the variability in evapotranspiration (Fig. 2c). Daily ET estimates at

the three sites were computed via the Food and Agriculture Organization of the United Nations (FAO) method (Allen et al. 1998). Cumulative daily ET over 2004 differs markedly as a result of the difference in land surfaces (Fig. 2c), compared to an average cumulative value of approximately 340 mm over the period of 1998–2006 at the Gudmundsen Automated Weather Data Network (AWDN) site (Sridhar et al. 2006). The 2004 cumulative daily total ET showed that the WET valley contributed the most water vapor to the atmosphere (582.6 mm) followed by the DRY valley (276.1 mm) and DUNE (213.2 mm) site. It is interesting to note that the daily ET is consistently higher at the WET site compared to the other sites during the growing season here (from July to September; Fig. 2c) even when root zone soil moisture becomes depleted at the adjacent DRY valley (Fig. 2a). The annual precipitation deficit (ET − precipitation) for the WET valley indicates that 231 mm of additional water is returned to the atmosphere than is received as precipitation. At both the DRY and DUNE locations, however, precipitation is greater than ET (by 76 and 139 mm, respectively). With similar rainfall amounts over the period at all three sites, an outside source of moisture, such as groundwater, is likely contributing to the root zone moisture content at the WET valley. There is a noticeable increase in the 50-cm soil moisture at the DRY site by early October that is not observed at the DUNE location (Figs. 2a,b). Between 1 October and 31 December 2004, 27.1 mm of precipitation was recorded at the DRY site while 26.2 mm was lost to ET. Over the same period, the column-integrated soil moisture within the first 100 cm (the root zone) increased by more than 60 cm. This suggests that the DRY location is a recharge interdunal valley, whereby subsurface water contributes some additional soil moisture to the valley through the remainder of the year that was depleted during the growing season. In fact, Chen and Hu (2004) report that the average monthly depth to groundwater at an additional site at Gudmundsen is estimated to be within 2 m of the surface through much of the year, and this affects the soil moisture and evapotranspiration in the region. Moreover, the higher water table at the WET valley and at times the DRY valley (Fig. 2a) over 2004 provided additional moisture for evaporation into the atmosphere compared to the DUNE site (Fig. 2b), thereby more than doubling the total ET over the annual cycle.

Average precipitation over 2004 (Fig. 2d) depicts that most of the annual rainfall occurred during the early warm season, and resulted from individual events of short duration that traversed the region during the spring and summer months, often producing more than tens of millimeters of precipitation over a given day (Fig. 2d). The are small differences in the cumulative annual precipitation amounts at the individual sites, due to errors associated with measurement as well as the spatial heterogeneity associated with the nature of convective precipitation often observed during the warm season.

### *d. Analysis of the mean diurnal cycle*

Examination of the mean diurnal variation in surface (2.1 m) air temperature shows that the DUNE location was generally warmer, by about 1 K, compared to the interdune sites (Fig. 3a). Moreover, the DUNE site was generally warmer during the daylight hours by approximately 0.5 K. The DRY and WET locations were each cooler than the DUNE site during an average day, and tended to differ from one another by less than 0.1 K. Physically, as a larger proportion of the soil composition at the DUNE location consists of pure sand and lacks the denser vegetation found at the other locations, it more readily absorbs incoming radiation and warms the ground surface, resulting in warmer mean maximum daily temperatures. At nighttime, soil temperatures at DUNE cool more quickly than the valley sites (Fig. 3b), and as additional energy is emitted into the atmosphere, the air temperatures remain higher there, though the total amount of cooling is similar over the diurnal cycle (about 2 K). Moreover, the soils of the interdune valleys typically contain more soil water than the DUNE location, resulting in cooler average soil temperatures (Fig. 3b) and less mean diurnal variation. The temperature patterns of the DRY and WET valley sites are damped accordingly, and reflect the additional vegetation, less exposed soil, and the generally higher soil moisture contents found at each location.

The differences in atmospheric water vapor between the Sand Hills' sites are apparent on both the annual and diurnal scale. To compare the relative amounts of atmospheric water vapor at the three locations, the 2.1-m mixing ratio (not shown) and vapor pressure deficits were examined (Fig. 3c). Little variation in the annual mean mixing ratio was noted between the locations throughout 2004, with differences of less than about 1 g $kg^{-1}$ (not shown). However, the atmosphere at the WET valley contained more water vapor during the green-up period in the spring months and during late summer (cf. Fig. 2c), likely due to additional transpiration and the effect of the higher water table on bare soil evaporation. These differences were on the order of 0.1 g $kg^{-1}$. Over the remainder of the year, the atmosphere at the DUNE site contained the least atmospheric water vapor. These results match the trends in the annual ET depicted above (Fig. 2c), and confirm

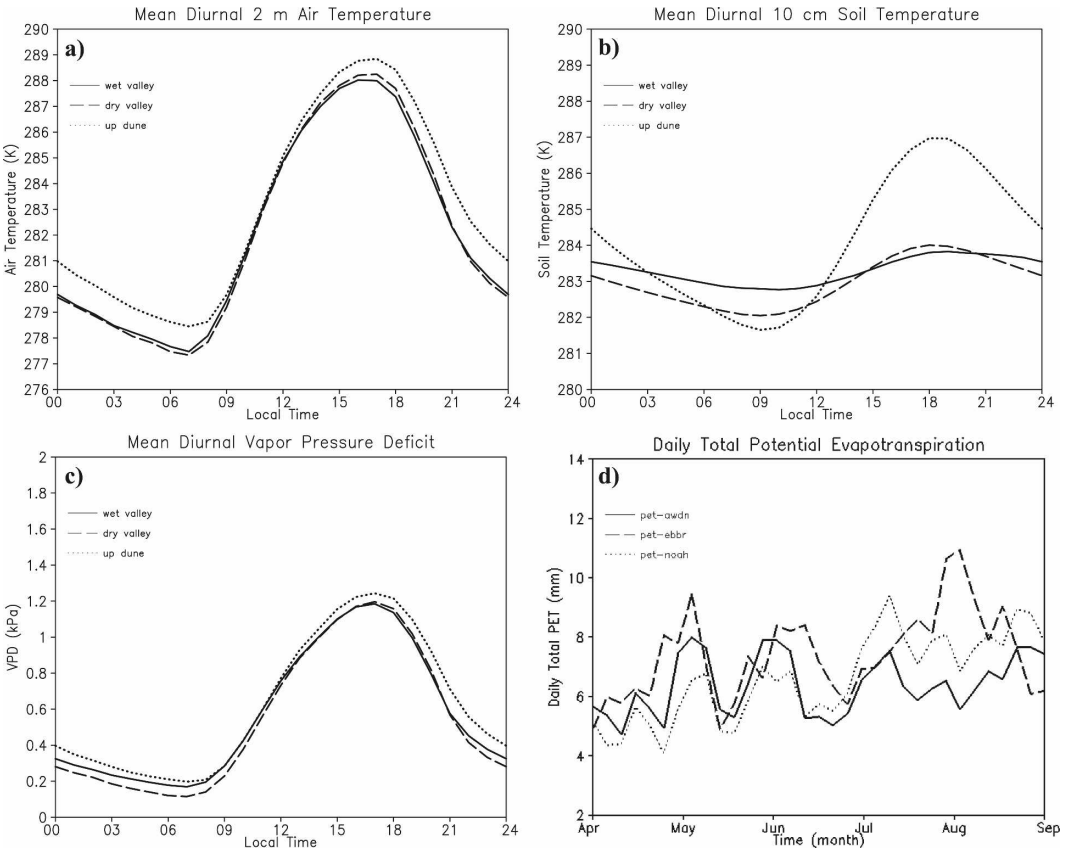


FIG. 3. (a) Observed mean diurnal 2-m air temperature (K) for the Sand Hills locations. (b) Same as in (a), but for the 10-cm soil temperature. (c) Same as in (a), but for the vapor pressure deficit (kPa). (d) Daily potential evapotranspiration (mm) at the AWDN, EBBR, and Noah LSM model run at the DRY location.

the observational and modeling study of Adegoke et al. (2003), where areas dominated by a greater vegetation fraction were typically cooler and moister then their nonvegetative counterparts. Further inspection of the mean diurnal vapor pressure deficit (Fig. 3c), indicates that the relative demand for water vapor is typically not met by late afternoon at the DUNE location. This deficit suggests that available soil moisture is quickly depleted from the sandy soils here, and plants quickly become stressed, resulting in less ET relative to the two interdune sites. It is hypothesized that the higher water table found frequently at the WET valley and seasonally at the DRY valley are the main mechanism responsible for supplying additional soil moisture to the root zone for use in ET.

## 3. Model description and experimental design

### *a. Description of the Noah LSM*

The Noah LSM version 2.7.1 (Ek et al. 2003) simulates soil moisture, soil temperature, surface skin temperature, plant canopy water content, snowpack, and surface energy and water flux terms in the context of their respective budgets and has been used in other experiments to examine the interaction between the land surface and atmosphere (Chen and Dudhia 2001a; Sridhar et al. 2002). The full descriptions of the fundamental equations of soil moisture hydrology and soil thermodynamics used in the current version of the Noah LSM are described in detail in Mahrt and Pan (1984), Mahrt and Ek (1984), and Chen and Dudhia (2001a).

Half-hourly averaged meteorological variables from the EBBR towers from 2004 were used to force the Noah LSM to test the model's ability to capture the fluxes and further assess the atmospheric differences at the three Sand Hills' locations. In particular, values of air temperature, humidity, wind speed, pressure, precipitation, and downward solar radiation were used directly from observations to force the model. The eighth variable needed to drive the model, downward longwave radiation, was not measured directly but was computed using an empirical estimate for atmospheric

TABLE 1. Soil and vegetative properties used in each simulation of the Noah LSM model runs. See text for the origin of each parameter.

| | Up dune (pure sand) | Wet valley (sandy loam) | Dry valley (sandy loam) |
|---|---|---|---|
| Saturated water content: $\Theta_s$ ($m^3\ m^{-3}$) | 0.339 | 0.434 | 0.434 |
| Saturated hydraulic conductivity: $K_s$ ($m\ s^{-1}$) | $4.66 \times 10^{-5}$ | $5.23 \times 10^{-6}$ | $5.23 \times 10^{-6}$ |
| Saturated soil suction: $\psi_s$ (m) | 0.070 | 0.141 | 0.141 |
| Empirical exponent: BB | 2.790 | 4.740 | 4.740 |
| Field capacity: $\Theta_{ref}$ ($m^3\ m^{-3}$) | 0.236 | 0.312 | 0.312 |
| Wilting point: $\Theta_{wilt}$ ($m^3\ m^{-3}$) | 0.010 | 0.040 | 0.040 |
| Quartz content (%) | 95 | 60 | 60 |
| Vegetation type | Grass | Grass | Grass |
| Vegetation fraction | 0.01–0.60 | 0.10–0.95 | 0.10–0.75 |
| Bottom layer soil temperature (K) | 283 | 283 | 283 |
| Soil heat capacity ($J\ m^{-3}\ K^{-1}$) | $1.28 \times 10^6$ | $1.28 \times 10^6$ | $1.28 \times 10^6$ |

emissivity as a function of air temperature and ambient vapor pressure (Sridhar and Elliott 2002):

$$\mathrm{LW}_{\mathrm{down}} = 1.40\left(\frac{10e}{T}\right)^{(1/7)}\sigma T^4, \tag{2}$$

where $\sigma$ is the Stefan–Boltzmann constant, $T$ is the air temperature (K), and $e$ is the vapor pressure (kPa). The coefficient (i.e., 1.40) in (2) was adjusted from the original value (i.e., 1.31) given in Sridhar and Elliott (2002) to minimize the error associated with the observed values of net radiation for all three Sand Hills' sites.

### b. Experimental setup

Parameter estimation for the vegetation and soil properties was achieved through a variety of methods. Soil parameters (Table 1) were largely based on available field data or estimated through the empirically derived equations of Cosby et al. (1984). Values for the field capacity ($\theta_{ref}$) and wilting point ($\theta_{wilt}$) for each soil type used were given in Chen and Dudhia (2001a).

As the WET and DRY sites were identified as containing sandy loam soil (option 3; Mitchell et al. 2001) and the DUNE site pure sand soils (D. B. Loope 2005, personal communication) adjustments were made (Table 1) to the values of the quartz content and saturated hydraulic conductivity (V. Zlotnik 2005, personal communication) relative to the predefault values found in the model. In addition, the total depth of the Noah LSM soil layers was set to 2 m, and the root zone was confined to the upper 1 m. Vegetation-type parameters were based on the values for the "ground cover" (e.g., grass, option 7) classification of Mitchell et al. (2001), which was derived from 1-km satellite data. The leaf area index of the vegetation was set to the default constant (i.e., 5.0) and the green vegetation fraction (GVF) in the Noah LSM is a monthly-variant parameter that is updated on the 15th day of each month. To estimate GVF for the three Sand Hills' locations, the method of Gutman and Ignatov (1998) was employed. Gutman and Ignatov (1998) derived a relationship between the GVF and satellite-based normalized difference vegetation index (NDVI) for use in weather models. This relationship is given as

$$\mathrm{GVF} = \frac{(\mathrm{NDVI} - \mathrm{NDVI_o})}{(\mathrm{NDVI_\infty} - \mathrm{NDVI_o})}, \tag{3}$$

where the subscripts "o" and "∞" denote a bare soil and dense green pixel value. Archived 2004 monthly 1-km NDVI data from the U.S. Department of Agriculture (USDA) were used for the three locations to derive the NDVI, $\mathrm{NDVI_o}$, and $\mathrm{NDVI_\infty}$ values. NDVI values were subjectively estimated by use of the nearest adjacent pixels to each observing location for each month. $\mathrm{NDVI_o}$ and $\mathrm{NDVI_\infty}$ were the minimum and maximum pixel values, (0.05 and 0.6, respectively) noted throughout all of 2004 and remained constant in computing the GVF using (3). Vegetation type remained constant throughout the model simulations.

The model was initialized at 0000 local time (LT) 1 January 2004 and run for 366 days in 30-min time steps, and the model was cycled through a 5-yr spinup period before analysis. Four soil layers were used for each model run, with thicknesses of 0.2, 0.1, 0.4, and 1.3 m, respectively, from the surface downward. This configuration was used so that the center points of each model soil layer in the root zone matched up directly with the observations of soil moisture and soil temperature. The initial conditions used for the soil moisture and soil temperature were based on the observed values where available, and linearly interpolated to match the observed depths. Missing data for the WET site were also linearly interpolated between the nearest available observed data point to complete the time series. The bot-

tom soil temperature for each model run was set to the mean annual air temperature at Mullen, Nebraska, from 1961 to 1990 for each location (283 K) as suggested in Mitchell et al. (2001). This location was chosen due the length of the temperature record and its close proximity to the EBBR sites.

## 4. Noah model evaluation

### a. Independent station verification

To provide a more robust assessment of the Noah LSM's ability to capture the diurnal and annual energy budgets at the Sand Hills locations, an independent analysis was performed with data not used to force the LSM. One year of meteorological data was obtained from the High Plains Regional Climate Center (HPRCC) AWDN for comparison with the EBBR DRY location (Hubbard et al. 1983). The Gudmundsen AWDN site most closely identifies with the EBBR DRY location in terms of proximity and vegetation, compared to the WET and DUNE sites, and does not constitute a location where subsurface water has a significant impact on the annual soil moisture profile based upon vegetation and soil moisture trends. The AWDN meteorological observing station at Gudmundsen records hourly averages of air temperature, relative humidity, precipitation, wind speed and direction, and solar radiation at a height of 1.5 m. Daily total PET (using a modified Penman method; Hubbard 1992) was recorded at the AWDN station and also computed for the EBBR site using the same method:

$$\mathrm{PET} = \frac{\dfrac{\Delta}{\Delta+\gamma}(R_n - G) + \dfrac{\gamma}{\Delta+\gamma} f(U)(e_s - e)}{\rho_w L_V}, \qquad (4)$$

where

$\Delta$ = slope of the saturation curve
$L_V$ = latent heat of vaporization
$\rho_w$ = density of water
$\gamma$ = the psychometric constant
$f(U) = 1.1 + 0.017(u)$, $u$ is the mean wind speed
$e_s$ = saturation vapor pressure
$e_a$ = actual vapor pressure,

and compared with daily PET output from the Noah LSM [which was computed using the modified Penman PET given in Mahrt and Ek (1984)]. PET was selected as the variable of interest to compare because of its inclusion of such state variables as temperature, moisture, and wind. Scalar errors of measurement were computed to assess model predictive capability including the mean absolute error (MAE).

Average daily totals of PET over the warm season (April–September, $n$ = 184 days) relate that the AWDN site ($\mathrm{PET_{AWDN}}$, 6.24 mm) was about 0.96 mm lower than the EBBR-derived PET ($\mathrm{PET_{EBBR}}$, 7.20 mm) and was slightly lower than the Noah LSM simulation ($\mathrm{PET_{NOAH}}$, 6.48 mm, Table 2). Of note as well is the greater variability (standard deviation) of the $\mathrm{PET_{EBBR}}$ (4.30 mm) compared to $\mathrm{PET_{AWDN}}$ (2.58 mm) and $\mathrm{PET_{NOAH}}$ (2.70 mm). This is likely due to the number of missing observations relative to the model output and AWDN data, each of which had a nearly complete dataset over the period. In addition, the MAE is less than 1 mm between the EBBR site and the Noah LSM model run, and there is a 0.22-mm difference between the AWDN and the Noah LSM model run. The general temporal trends and variation in magnitude among the various PET estimates are similar from April to September (Fig. 3d). The consistency noted with the PET between the two "DRY" observing stations and the model indicate that the model forcing via the DRY site data is representative of the actual atmospheric trends in the area.

TABLE 2. Independent model validation statistics for the AWDN site, DRY EBBR site, and Noah LSM dry valley model simulation.

| $N$ = 184 days | AWDN station | EBBR DRY valley (AWDN method) | DRY valley Noah simualtion |
|---|---|---|---|
| $\bar{x}$ (mm) | 6.24 | 7.20 | 6.48 |
| $s_x$ (mm) | 2.59 | 4.30 | 2.70 |
| MAE (mm) | 0.22 | 0.96 | |

### b. Annual and diurnal trends of the energy budget

The observed mean diurnal cycle analysis depicts the partitioning of the net radiation in (1) at all three Sand Hills' sites (Figs. 4a, 5a, and 6a) and the influence of subsurface water at the WET site is evident. As expected, the net radiation trends were similar, with peak values of about 350–375 W $\mathrm{m^{-2}}$ by 1200 LT and minimum values near $-50$ W $\mathrm{m^{-2}}$, indicative of a net flux into the atmosphere during the overnight hours. Note that at the DRY valley (Fig. 5a) the peak net radiation is greater than the other two sites, due primarily to the concentration of available observations into the warm season. As a majority of the available observations here occurred during these months, the "annual" cycle at this location is biased somewhat toward summertime values, with only about one-half the number of data points used relative to the WET valley and DUNE sites. Little diurnal variability of the ground heat flux ($G$) was noted at the WET (Fig. 4a) and DRY locations (Fig. 5a), with differences of less than 20 W $\mathrm{m^{-2}}$ and peak values occurring in late afternoon.

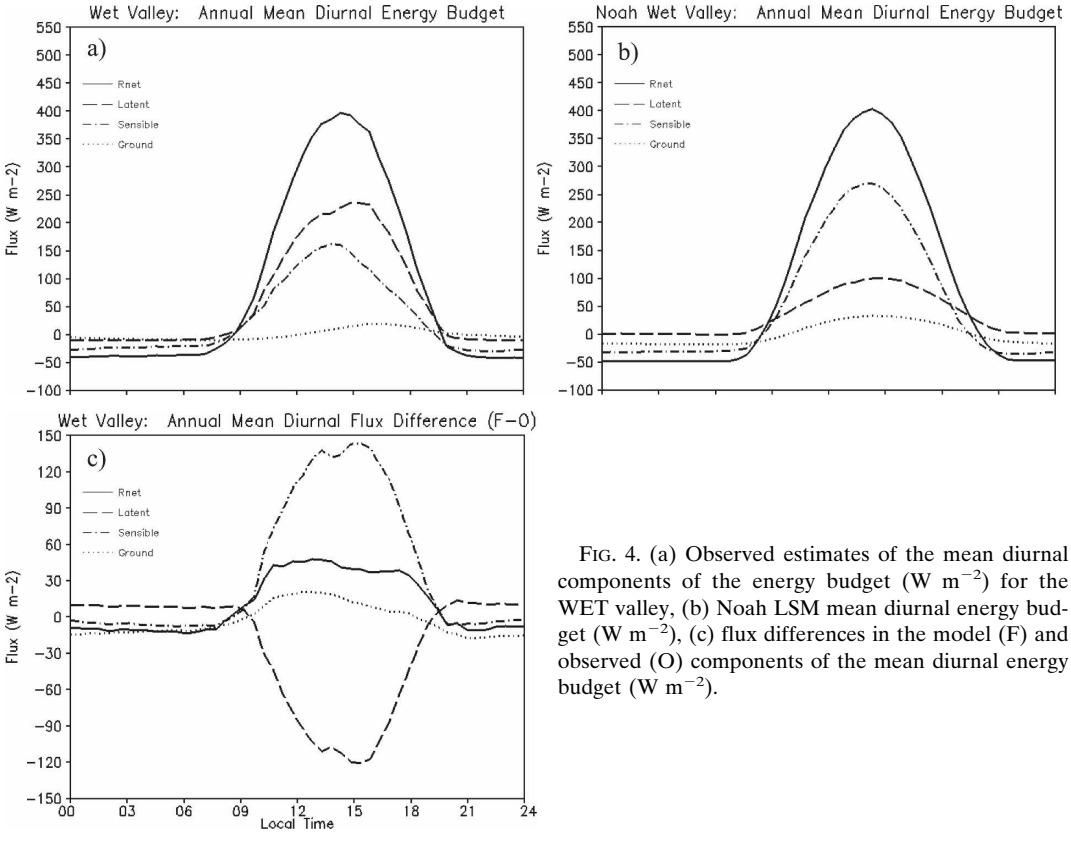


FIG. 4. (a) Observed estimates of the mean diurnal components of the energy budget (W $m^{-2}$) for the WET valley, (b) Noah LSM mean diurnal energy budget (W $m^{-2}$), (c) flux differences in the model (F) and observed (O) components of the mean diurnal energy budget (W $m^{-2}$).

At the DUNE location, there was greater diurnal variation in $G$ with peak values near 50 W $m^{-2}$ occurring around 1500 LT (Fig. 6a), several hours earlier than at either the WET or DRY valley locations. Because of the relatively sparse vegetation, lack of groundwater, and dry soils near the surface of the DUNE site compared to the companion sites, the bare soil was able to more quickly absorb incident radiation and conduct thermal energy across the soil flux plate during the day. At night, the DUNE location averaged lower values of soil heat flux by 10–20 W $m^{-2}$, indicating that more energy is used in heating the surrounding atmosphere (and soil underneath), relative to the valley sites, which is also reflected in the diurnal air temperature cycle (Fig. 3a).

Sensible ($H$) and latent heat flux estimates (LE) among the three sites differed over the mean diurnal cycle. At the WET valley location (Fig. 4a), peak-estimated LE values that approached 250 W $m^{-2}$ were noted by early afternoon as compared to 225 W $m^{-2}$ at the DRY and 75 W $m^{-2}$ at the DUNE locations. This is to be expected, as additional soil moisture from the higher water table at the WET site was likely responsible for the increased values, and contributions from bare soil evaporation and plant transpiration are greater here. The estimated LE value at the DRY site is biased high, due to the period of observation, and comparisons over the same time frame indicate that the estimated WET LE peaks at about 350 W $m^{-2}$. There was also a small lag of about 1 h in the estimated LE peak compared to the $H$ peak flux at each of the valley locations compared to the DUNE site. This was likely due to the extra time required for the plants to reach an optimum transpiration temperature by early afternoon. In addition, while peak-estimated LE values at the WET and DRY locations occurred at approximately the same time, there was a noticeable shift of a few hours in peak values at the DUNE site to near local noon (Fig. 6a). The discrepancy in the estimated LE at the DUNE site may be the result of additional plant stress here, limiting transpiration as soil moisture in the root zone is depleted quickly after sunrise along with a lack of influx of soil moisture from an underground source as in the valley sites. The DRY site exhibited the greatest diurnal range in $H$ (Fig. 5a), even when the DUNE site data series was corrected for the missing cold season data at the DRY site (not shown). Values of $H$ peaked at 250 W $m^{-2}$ at midday here and at 225 W $m^{-2}$ at the DUNE location (240 W $m^{-2}$ when cold season data was omitted). As expected, with less soil

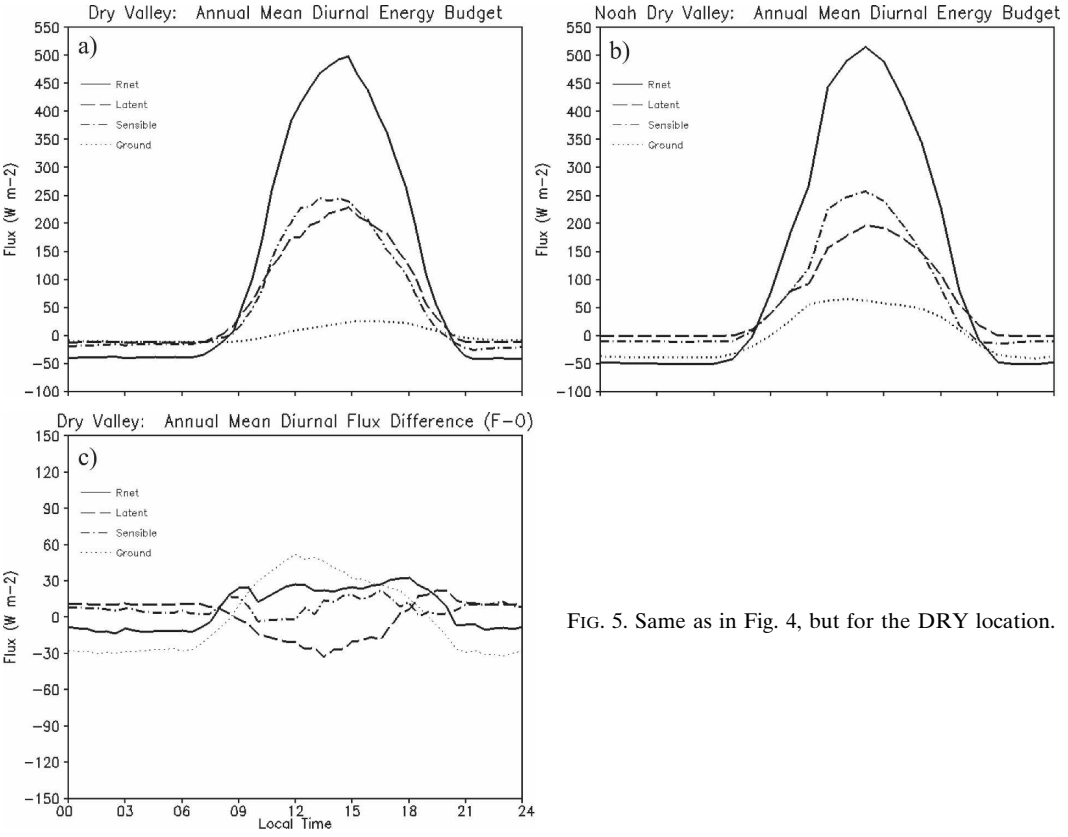


FIG. 5. Same as in Fig. 4, but for the DRY location.

moisture and plant transpiration at these sites, more energy was available for heating of the air. Conversely, the WET location exhibited the smallest $H$, with peak midday values near 175 W m$^{-2}$ (Fig. 4a).

The Noah LSM performed reasonably well at the DRY and DUNE locations in capturing the mean diurnal energy budgets without any adjustment for the influence of the water table, but exhibited some difficulty at the WET site (Figs. 4b, 5b, and 6b). With a similar amount of net radiation received at each location, energy was partitioned differently between LE and $H$, depending on the soil and vegetative properties of the location. Numerous other studies have statistically examined the ability of the Noah LSM (or some derivative) to reproduce surface fluxes, including Chen and Dudhia (2001b), Sridhar et al. (2002), and Evans et al. (2005). Evans et al. (2005) report that the Noah LSM (MM5/OSU version) coupled to a regional climate model overestimated $H$ and underestimated LE over their study period. They attribute the discrepancy in LE to an underestimation of the ET over the model integration, similar to our results for the WET location. They also note that $H$ is consistently overestimated, as the lack of ET results in warmer soil and surface skin temperatures thereby artificially increasing $H$. Conversely, Sridhar et al. (2002) report that for several sites in Oklahoma, both $H$ and LE were overestimated by the model, as noted in the DUNE simulation.

For the "sources" of $H$ and LE, an overestimation in the available energy ($R_{\text{net}} - G$) was generally noted in all three model runs (Figs. 4b, 5b, and 6b), particularly during peak afternoon heating at the WET and DUNE locations. Errors in net radiation occurred mainly during midday and during the warm season, with a typical range of between 10–40 W m$^{-2}$ over the three sites. It is likely that the estimations of the "observed" incoming longwave radiation computed from (2) and used in the model was the cause. At all locations, the magnitude of the modeled ground heat flux during the day was greater than the observed values, while typically less at night. This was likely due in part to the overestimation of $R_{\text{net}}$ in addition to the increased diurnal range in soil temperatures. Moreover, as noted earlier, a correction of about 15–40 W m$^{-2}$ for the difference in surface and 0.1-m soil flux would further close the gap between the observed and modeled values.

In the WET simulation (Fig. 4b), the modeled available energy is distributed less evenly among $H$ and LE as compared to the observed values. Peak values of

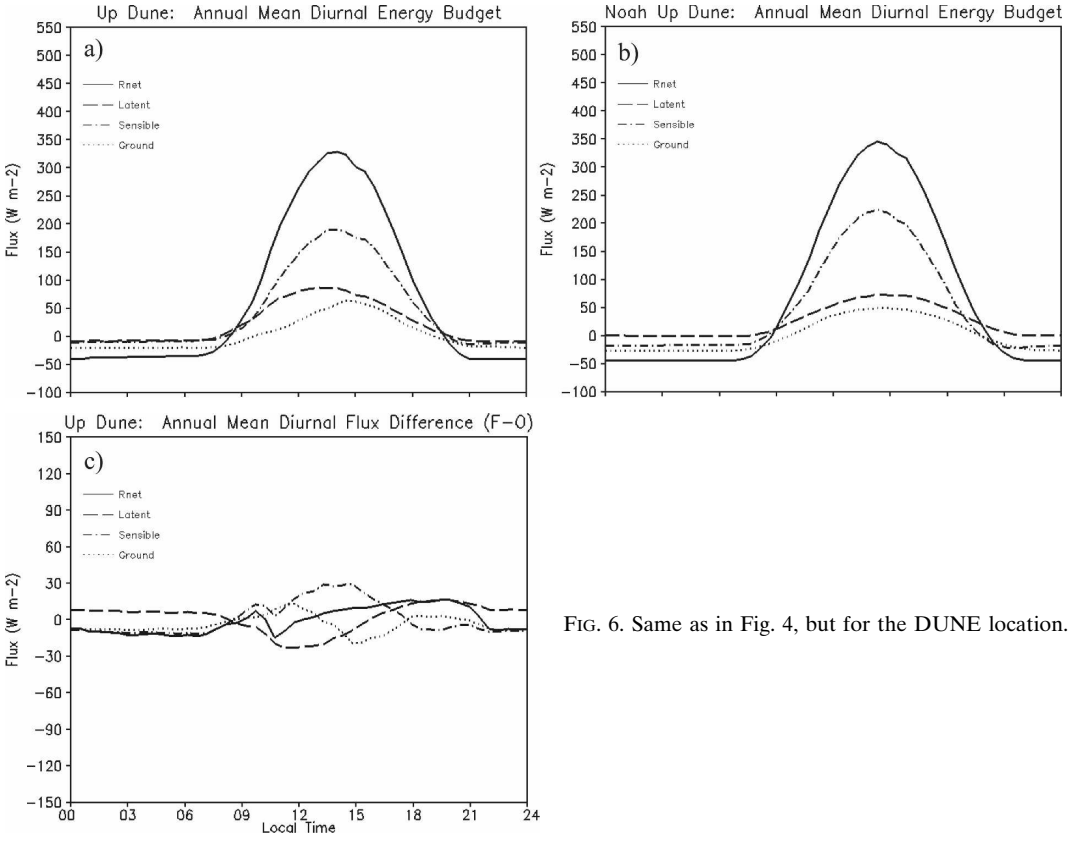


FIG. 6. Same as in Fig. 4, but for the DUNE location.

modeled LE and $H$ are estimated at 125 and 275 W $m^{-2}$, respectively, compared to the observed values of 250 and 175 W $m^{-2}$. Clearly, the model exhibits some difficulty in capturing these peak values. The timing of peak values of the $H$ and LE are similar, occurring at 1300 LT for $H$ and 1400 LT for LE (Fig. 4c). Differences over the diurnal cycle depict slight shifts in the timing of peak values. For example, LE decreases much more slowly in the Noah LSM simulation from 1500 to 1800 LT, causing an increase in the error (Fig. 4c) during that time interval. The Noah LSM soil heat flux at the WET valley exhibits a shift in the timing of peak values as well as a difference in magnitude over the diurnal cycle (Fig. 4c). Greater diurnal variation is noted, with an earlier occurrence of peak values of 45 W $m^{-2}$ at 1500 UTC as compared to the peak observed flux of 25 W $m^{-2}$. The model overestimates the ground heat flux during the day and overnight (Fig. 4c). The differences are likely due to the model's inability to accurately represent the WET valley soil environment over the year. Thus, the modeled ground heat flux values are "enhanced" compared to the observations, as the lack of additional soil water from another source (such as groundwater) permits a greater daily exchange of energy from the soil to the atmosphere.

Over the annual cycle (not shown), the largest errors of $H$ and LE in the model simulation occur during the late warm season, when precipitation is much more sporadic and subsurface water contributions to soil moisture are at a maximum. The Noah LSM tends to overestimate LE from January to March, when a steep decline is noted through July when the LE is underestimated until mid-October in the model (when recharge at the DRY valley is observed to occur; Fig. 2a). This suggests that by midsummer, there is another source of available soil moisture for the bare soil evaporation and plant transpiration that contributes to LE at the WET EBBR site, but is not well represented in the Noah LSM. While no soil moisture observations are available for this location to verify with a specific degree of certainty, it has been shown that groundwater is likely contributing to the soil moisture here (Gosselin et al. 1999; Chen and Hu 2004). As the Noah LSM does not currently account for water sources such as groundwater or lateral drainage into the soil, it can lead to an erroneously dry soil moisture profile over long periods, such as we have shown, as well as an inaccurate partitioning of the surface energy budget, which is likely the case here. This suggests that some incorporation of subsurface water into the Noah model would improve the

soil moisture profile here and result in a more accurate estimation of the surface fluxes.

The model results of the DRY (Fig. 5b) simulation are similar to those of the WET run, though there are differences. Over the diurnal cycle (Fig. 5b), greater energy went into H and less into LE in the Noah LSM than the observations. The Noah LSM underestimated LE by 20–30 W $m^{-2}$ by 1300–1700 LT (Fig. 5c). At the same time, $H$ was overestimated by local noon, approaching differences of 10–20 W $m^{-2}$. As in the WET site, the modeled ground heat flux at the DRY valley exhibited a greater mean diurnal range than the observations, spanning between $-75$ W $m^{-2}$ during the overnight hours to 45 W $m^{-2}$ during peak afternoon heating. Again, the Noah LSM model tends to overestimate the ground heat flux during the day and at night (Fig. 5c), indicative of the model's inability to represent the wetter soils found at the DRY site, particularly at depth during the warm season, and thus exchanges too much energy with the atmosphere.

Over the annual cycle (not shown), a seasonal trend is clearly noted. During the cool season, from November to March, both LE and $H$ are slightly underestimated by the Noah LSM; $H$ more so than LE. Earlier in the year, the Noah LSM rapidly dries out the soil moisture, particularly at lower depths, as compared to the observations (not shown) by late spring. This in turn reduces the soil moisture availability within the root zone and allows for continuous drainage of soil moisture through the lowest layers, reducing the amount of soil water available for ET. Thus, at this site where subsurface water appears to influence the soil moisture greatest during early spring and fall (refer to Fig. 2a), the largest model errors in $H$ (overestimated) and LE (underestimated) are noted between July and October, due to the model's inability to represent the wettest soils at depth earlier in the year, and this error propagates through the summer.

The DUNE site (Fig. 6b) resulted in the best simulation over the diurnal and annual cycle. This "improvement" was likely the result of fewer influencing factors such as vegetation and subsurface water, which are found at both valley locations. Observed and modeled net radiation and ground heat fluxes in the diurnal cycle were strikingly similar in magnitude. Net radiation peaked at 350 W $m^{-2}$ for both the observed and model values. The differences in the ground heat flux between the simulation and observations were near 50 W $m^{-2}$, and the peaks occurred similarly, at about 1500 LT. There was a slight increase in the time it took the ground heat flux to achieve a peak value in the simulation, suggesting that the model soil warmed more rapidly than in reality. The quick nature by which the soil appears to warm and produce a higher ground heat flux is a consistent bias that was noted throughout all Noah LSM simulations.

Fluxes of $H$ and LE at the DUNE site exhibited little error over the mean diurnal cycle (Fig. 6c) as compared to the valley locations. Modeled values of $H$ at peak heating here are 225 W $m^{-2}$ compared to an observed value of 200 W $m^{-2}$. For the peak in LE, there is little overall difference in the diurnal cycle, with 100 and 70 W $m^{-2}$ for the observed estimated and simulated values, respectively. There is a shift in timing of these peak values, however. Estimated observed LE peaks occur near 1300 LT, while in the Noah LSM, the highest values occur at 1500 LT. Annual analysis of $H$ and LE does not depict a clear bias, as in the WET and DRY locations (not shown). There is a slight model overestimation of LE from September to December and model underestimation of $H$ over the same period, but no clear annual pattern in the errors during the mid–late-summer period. This lack of a distinct pattern suggests that unlike the valley sites, the absence of treatment of subsurface water in the Noah LSM model does not affect the resulting surface fluxes here, and associated errors result instead from errors with only the model physics and parameterization of the soil properties.

### *c. WET and DRY valley soil moisture comparisons*

To investigate further the influence of subsurface water on the WET and DRY valley soil moisture, an examination of the modeled and observed root zone profiles is presented (Fig. 7). Some of the error in the modeled sensible and latent heat fluxes can be attributed to errors in the modeled soil moisture profile as a result of the prescribed Noah LSM soil moisture dynamics or model parameterization, and may not be due solely to the model's absence of a near-surface water table. As soil moisture is an influencing factor to the partitioning of the surface energy budget, an annual comparison depicts differences between the modeled and observed values (Fig. 7). At the DRY site, where subsurface water is less influential over the year compared to the WET valley (see Gosselin et al. 1999), errors in the model soil moisture are evident, particularly during the warm season. This suggests that discrepancies in the parameterization of the model soil properties or in the model soil moisture dynamics do, in fact, compose some portion of the total error in the soil moisture profile at this location. The Noah LSM tends to underestimate the soil moisture during most of the year here (Fig. 7), particularly during the growing season when demand for soil water is high and precipitation wanes, especially from June to August. This ap-

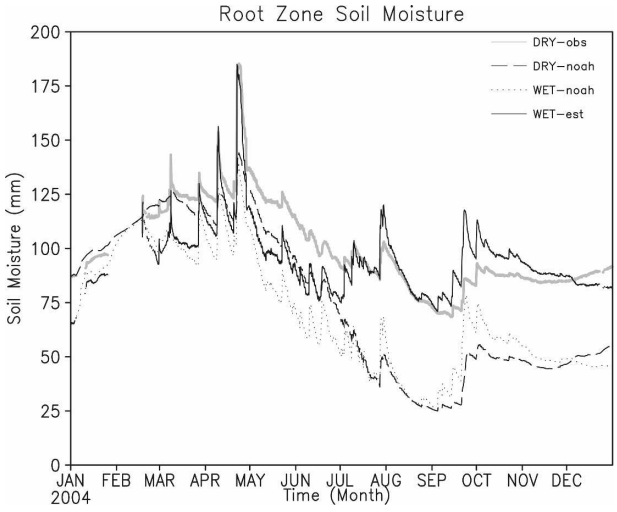


FIG. 7. Column-integrated soil moisture through a depth of 50 cm for the WET and DRY valleys. Gray curve is the observed values at the DRY valley. The Noah LSM soil moisture is given by the dashed line for the DRY site and the dotted line for the WET site. Solid black curve indicates the modeled WET valley soil moisture adjusted for errors only due to the model soil moisture dynamics.

pears to result from the Noah LSM's inability to account for the high soil moisture content at depth earlier in the year, when subsurface water is a factor prior to the onset of the growing season in March and April, and the error continues through the entire model integration. As mentioned earlier, there is a distinct error in the modeled 80-cm soil moisture at the DRY site, whereby a continuous decrease is noted early in the season (but not in the observations) and this is reflected in the large errors in the modeled sensible and latent heat fluxes during the late summer. There is also a noticeable difference in the October–December time frame, when recharge of soil moisture from below is apparent at the DRY valley, exhibited by the lack of precipitation after mid-October (Fig. 2d) and the increasing root zone soil moisture (Fig. 7). At the WET site, no soil moisture data were available, and the modeled soil water content (dotted curve) is consistently less than the DRY site for most of the year, due to the increased modeled vegetation fraction here. As subsurface water is less important annually at the DRY site—at least during the growing season—one can assume that errors in the modeled soil moisture profile here are due only to errors in the parameterization of the soil dynamics. Since the model design for the WET and DRY sites are similar in terms of parameterization of soil properties (see Table 1), one can use the difference between observed and modeled soil water in the root zone of the DRY site as a correction for the errors due to only the parameterization of the soil hydrology at the WET site. This is achieved by adding this difference to the modeled root zone soil moisture at the WET site for an approximation of the "true" soil moisture without any subsurface water influence (Fig. 7 solid black curve labeled "WET-est"). The new observed soil moisture at the WET site remains less than that of the DRY site until late July and again from mid-November to December, though indirect evidence, such as higher green vegetation fraction and the existence of the drainage ditch as pointed out in Gosselin et al. (1999), relate that the soils at the WET site contain a higher soil moisture content. The observations of daily ET from both valley sites (Fig. 2c) also show that WET valley ET is greater than DRY valley ET throughout 2004. This suggests that any errors associated with the model parameterization of the soil hydrologic properties in the Noah LSM at the WET site can only partially explain the errors in the modeled and observed soil moisture profiles and the surface fluxes. At the WET valley, an additional outside factor must contribute to the soil moisture throughout the year and ultimately affect the surface fluxes.

The variation of soil moisture content and latent heat flux over a subannual time period is also examined to assess the soil moisture response to a precipitation event (Fig. 8). Approximately 6 and 12 cm of precipitation fell at the DRY and WET locations, respectively, during the evening and early morning hours of 29–30 July 2004. Observed soil moisture in the root zone increased at the DRY site immediately following the onset of precipitation (dotted line) and the DRY run of the Noah LSM responded similarly, though soil moisture content increased more gradually over a longer period of time in the model, suggesting a discrepancy in the unsaturated hydraulic conductivity. It is also worth noting on this time scale that, while the model underestimates the soil water content at the DRY valley before and after the precipitation event (see Fig. 7), soil moisture decreases at approximately the same rate during the entire period. The WET Noah LSM model run (solid gray curve) also responds predictably, with a greater increase in soil water content than in the DRY run due to the higher precipitation amount and lower initial soil moisture content. The rate of soil moisture decrease is nearly the same as in the DRY model run and the DRY observed values, with 3–4 mm of soil moisture depleted from the soil over the 3 days following the rainfall event.

The EBBR latent heat fluxes (Fig. 8b) for both the WET (solid gray) and DRY (black dashed) site appear to follow a very similar pattern, and do not change significantly after the precipitation event. Observed LE

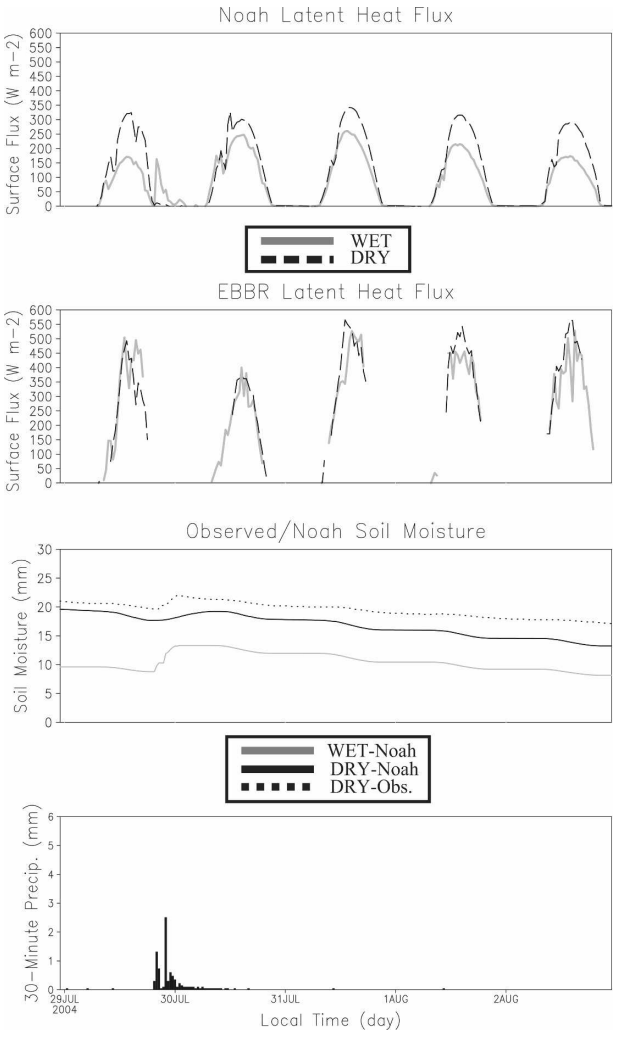


FIG. 8. The response of observed and modeled 10-cm soil moisture and latent heat flux to a summer precipitation episode. The plotted precipitation histogram is an average of both the WET and DRY valley observed 30-min values.

peaks at approximately 500 W $m^{-2}$ on 29 June 2004 and falls to 400 W $m^{-2}$ the following day during the precipitation event. On the day after the rain, observed LE at both locations is slightly higher than on 29 June 2004, with maximum values at each site nearing 550 W $m^{-2}$. Even with almost twice the precipitation of the DRY site, little variation in maximum EBBR LE is noted over the next 2 days at the WET site. However, the DRY valley site has maximum LE greater than for the WET site following the event, and exhibits a larger increase. This implies that isolated precipitation events may impact the partitioning of the surface energy budget at the DRY site more than at the WET site, where the higher soil moisture contents tend to buffer the impact of singular precipitation events. This is not reflected in the Noah LSM simulations. With less root zone soil moisture by late July 2004, the WET Noah LSM model run continued to exhibit lower LE, even after the precipitation event, than the DRY model run (Fig. 8). While LE is underestimated for both these model runs, the larger error clearly lies with the WET run, with continuing reductions in maximum LE over time compared to the EBBR LE estimates. This suggests that the Noah LSM is not accounting for an outside source of soil moisture, and the cumulative effect of the neglect of related processes since the beginning of the model is evident by late summer.

### *d. Annual model evaluation statistics*

To quantify the predictive capabilities of the Noah LSM at the Sand Hills' locations, scalar error statistics such as the mean bias error (MBE), MAE, and root-mean-square error (RMSE; Wilks 1995) were computed for the half-hourly values of the surface fluxes between the observations ($O$) and the model ($F$) (Table 3). The total number of data points used in the statistical summary (Table 3) varied somewhat due to missing or unavailable observations at each site. Overall, the DUNE location yielded the best simulation by the Noah LSM (Table 3), based on the MBE and MAE values. MAE values of 26.2 and 19.6 W $m^{-2}$ are noted for the DUNE $H$ and LE flux differences, which are within 15%–20% of the mean daily values. Most MAE values (Table 3) for the differences in the $H$ and LE fluxes were within 15%–25% of mean daily values, except for the WET site, exhibiting the Noah LSM's inability to account for the contributions from subsurface water here. In comparison, at the DRY valley site the modeled surface flux errors were on average 10% less and for the DUNE location they were 50% less than those of the WET location. A notable negative (positive) bias in the latent (sensible) heat flux is exhibited at the WET valley (Table 3), in conjunction with the diurnal and annual trends noted earlier and is likely due in part to the model's inability to accurately capture the soil moisture profile here and, ultimately, the LE.

### *e. Short time series analysis*

To examine model performance at a higher temporal frequency, short time periods for each of the three sites are examined under two general conditions: when errors in the model energy budget are relatively small and when they are relatively large (Table 4). To determine periods of "small" and "large" model errors, the 10-cm soil temperature over a 5-day period was used as a discriminator. At the WET and DRY locations, 29 July–2 August 2004 was chosen to reflect how the ab-

TABLE 3. Annual energy budget verification statistics for the performance of the Noah LSM for each of the Sand Hills location used in the study.

| $R_{net}$ | MBE = $[\Sigma_{i=1}^{n}(F - O)/n]$ (W m$^{-2}$) | RMSE = $\sqrt{[\Sigma_{i=1}^{n}(F - O)^2/n]}$ (W m$^{-2}$) | MAE = $(\Sigma_{i=1}^{n}\lvert F - O\rvert/n)$ (W m$^{-2}$) | $n$ |
|---|---|---|---|---|
| Wet valley | 11.6 | 44.6 | 32.1 | 11 243 |
| Dry valley | 6.70 | 48.7 | 32.8 | 5900 |
| Up dune | 0.50 | 33.8 | 24.8 | 13 151 |
| | | $H$ | | |
| Wet valley | 41.7 | 111.5 | 61.7 | |
| Dry valley | 5.79 | 67.0 | 42.6 | |
| Up dune | 2.85 | 39.2 | 26.2 | |
| | | LE | | |
| Wet valley | −27.7 | 94.6 | 48.2 | |
| Dry valley | −2.96 | 56.2 | 35.3 | |
| Up dune | 0.77 | 29.9 | 19.6 | |
| | | $G$ | | |
| Wet valley | −1.80 | 25.1 | 17.7 | |
| Dry valley | 5.45 | 40.4 | 30.6 | |
| Up dune | −3.60 | 25.1 | 17.1 | |

sence of an influx of subsurface water in the model corresponds to large errors in the model soil temperatures and surface flux estimates (Figs. 9 and 10). At the WET site, Noah LSM soil temperatures exhibit small error compared to the observations, both in magnitude and trend during late May (Fig. 9a). This is indicative of the soil water content remaining similar between model and observations, prior to the significant dry-down period of summer (see Fig. 2a). By early August (Fig. 9b), there is a consistent positive bias in soil temperature of about 1.5 K, which suggests that the reduced soil moisture in this model simulation permits the soils to warm too quickly on a diurnal basis, and exhibits greater variation in diurnal temperature. The drier soil results in larger surface flux error, with an underestimation of LE and an overestimation of $H$ compared to the observed flux estimates. Maximum flux differences of less than about 100 W m$^{-2}$ for $H$ and LE are noted in May (Fig. 9c) with much greater errors, on the order of 200–300 W m$^{-2}$ for the early August time frame, when the modeled soil water is artificially low (Fig. 9d).

At the DRY location a similar trend to that of the WET model simulation is seen, whereby 10-cm soil temperatures in late May (representing small flux errors) are more accurately modeled than during early August (Figs. 10a,b) after soil moisture depletion. A similar trend is also depicted in the surface fluxes here with RMSEs of $H$ and LE being much less in late May (Fig. 10c) than when the difference in soil temperatures are large by early August (Fig. 10d). In fact, from 31 July to 3 August, an apparent increase in soil temperature difference is reflected in the RMSE of the surface fluxes. It appears that at the DRY site errors in the soil moisture profile begin to occur during the early spring, when subsurface water influences the valley. As this process is not explicitly accounted for in the model, the errors in soil moisture and surface fluxes continue to propagate into late summer. Moreover, the large errors

TABLE 4. Summary statistics for short time series exhibiting small and large model errors. RMSE and NSE* are defined in the text and compare the model goodness of fit.

| Site/subperiod error | $R_{net}$ (RMSE/NSE) | Ground (RMSE/NSE) | Sensible (RMSE/NSE) | Latent (RMSE/NSE) |
|---|---|---|---|---|
| WET annual | 44.6/0.95 | 25.1/<1 | 111.2/0.53 | 94.6/0.49 |
| WET (small) 21–25 May | 34.5/0.99 | 13.5/0.58 | 67.2/0.62 | 55.7/0.85 |
| WET (large) 29 Jul–2 Aug | 45.9/0.97 | 11.4/0.55 | 171.8/<1 | 149.4/0.40 |
| DRY annual | 48.7/0.96 | 40.4/<1 | 67.0/0.69 | 56.2/0.78 |
| DRY (small) 21–25 May | 88.7/0.87 | 30.1/<1 | 68.0/0.71 | 64.0/0.77 |
| DRY (large) 29 Jul–2 Aug | 58.1/0.94 | 24.8/<1 | 130.6/<1 | 123.9/0.56 |
| DUNE annual | 33.8/0.96 | 25.1/<1 | 39.2/0.83 | 29.9/0.72 |
| DUNE (small) 9–13 Mar | 22.0/0.98 | 28.5/0.66 | 32.2/0.93 | 27.3/0.28 |
| DUNE (large) 21–25 May | 27.1/0.98 | 15.9/0.84 | 50.4/0.75 | 37.6/0.80 |

*NSE = $1 - (\Sigma_{t=1}^{N}(O_t - M_t)^2/\Sigma_{t=1}^{N}(O_t - \overline{O}_t)^2)$.

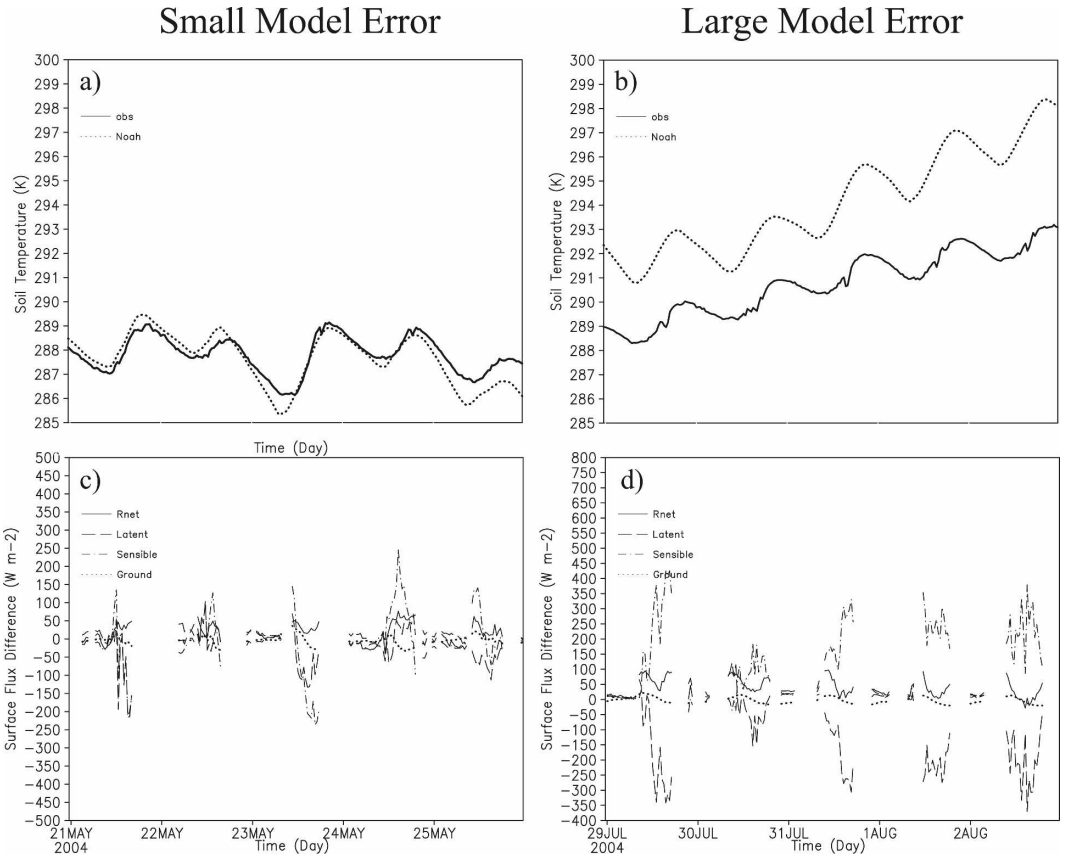


FIG. 9. WET 10-cm soil temperature for a case with (a) a small difference and (b) a large temperature difference. (c), (d) The surface flux estimate differences corresponding to (a), (b).

in the surface fluxes at the DRY site are consistently less than that of the WET site (Figs. 9d and 10d) indicating the important influence of subsurface water on the soil moisture profile at the WET site.

The overall trend at the DUNE site is much less clear, with no influence from subsurface water at any time of the year, resulting in a larger diurnal variation in 10-cm soil temperatures relative to the valley sites (Figs. 11a,b) and the observed soil temperature often greater than the modeled temperatures, indicating a cool model bias here. The magnitude of model errors of $H$ and LE in particular is much less than those of the valley sites (Figs. 11c,d). With differences in soil temperatures of 2–4 K, flux errors are predominately less than 50 W $m^{-2}$, smaller than at either the WET or DRY locations. This is attributed to the smaller and less varying amounts of soil moisture seen at this site during the year, and with no influence of subsurface water, the model is able to better represent the true state of the soil moisture profile and this is subsequently reflected in better estimates of the surface fluxes.

A quantitative assessment was also performed for each subperiod using the root mean squared error and Nash–Sutcliffe efficiency (NSE; Nash and Sutcliffe 1970) to compare with the annual evaluation statistics (Table 4). NSE values range between $-\infty$ and 1.0, with values of 1.0 indicating perfect model performance. At all three sites, $H$ is overpredicted and LE is underpredicted by the Noah model with error values between about 20 and 50 W $m^{-2}$ in most instances. As noted earlier, this is mainly due to errors associated with the computation of incoming longwave radiation used to force the Noah model. In general, the WET site exhibited the largest error in the modeled surface fluxes over the shorter time frames, with maximum RMSE values near 172 W $m^{-2}$ for $H$ and 150 W $m^{-2}$ for LE by early August (Table 4). This large error in LE was partially offset by a smaller error during late May (55.7 W $m^{-2}$), as compared to the annual RMSE (94.6 W $m^{-2}$) in LE. NSE followed a similar trend for both $H$ and LE, larger during the May period and smaller in early August relative to the annual values. The DRY site exhibits a similar trend with errors of smaller magnitude, though a larger error in net radiation is evident in each case.

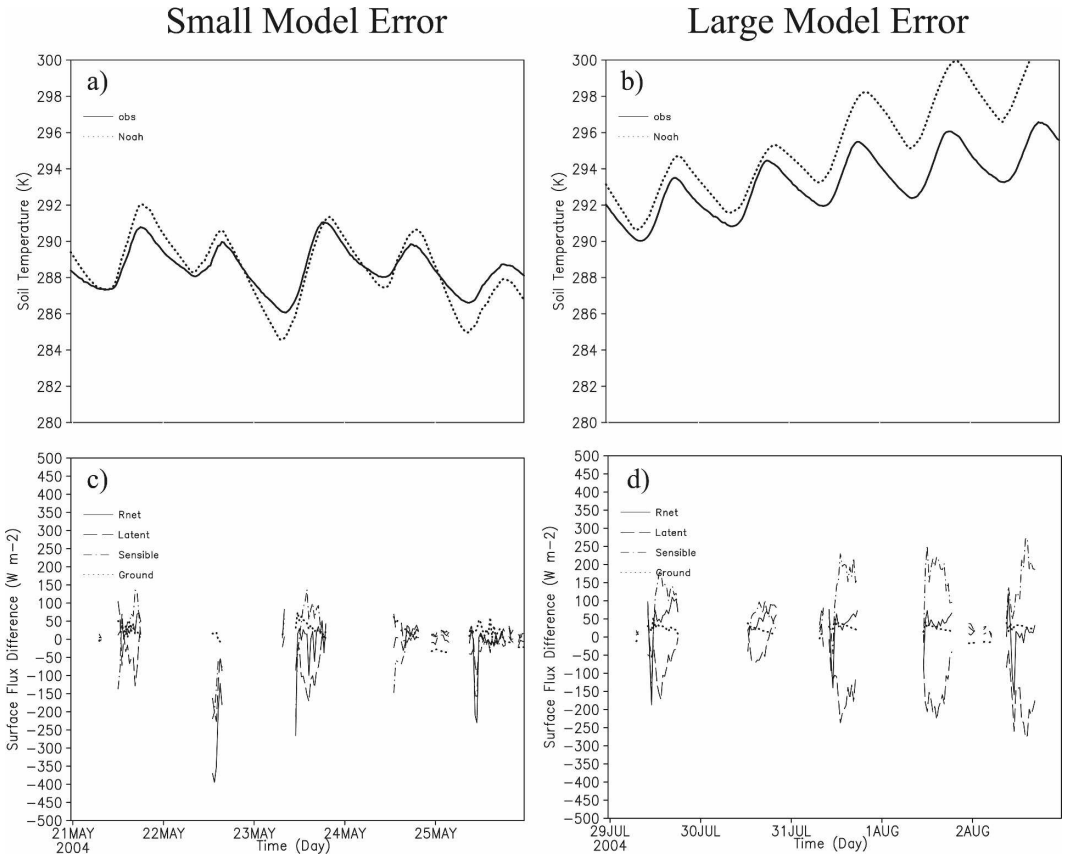


FIG. 10. DRY 10-cm soil temperature for a case with (a) a small difference and (b) a large temperature difference. (c), (d) The surface flux estimate differences corresponding to (a), (b).

DRY site $H$ and LE errors of nearly 130 W m$^{-2}$ for the late summer case (Fig. 10d) are close to those of the WET site. Sensible heat flux estimates are much too high in the Noah model, indicative of the lack of an additional soil moisture source for use in LE, and an artificially high soil temperature that translates into larger sensible heat flux values. As expected, the DUNE site yields the smallest model errors, as only a modest difference is noted between the annual and subperiod values.

## 5. Conclusions

The energy budgets at three locations in the Nebraska Sand Hills were examined to determine the influence of subsurface water on surface fluxes over annual and diurnal time scales. These three sites are in close proximity, share similar atmospheric forcing, and collectively represent the range of hydroclimatic conditions found in the region: an interdune valley heavily influenced by subsurface water (WET), an interdune valley seasonally influenced (DRY) by subsurface water (Gosselin et al. 1999; Chen and Hu 2004), and a dunal upland site (DUNE) not affected by the water table. While each site had almost identical net radiation, distinct differences were evident in the partitioning of the surface fluxes at each location, and these differences were tied to the variation of subsurface water. The WET location had the greatest amount of net radiation partitioned into latent heat flux, while the DUNE site had the least. Conversely, the DRY site had slightly greater net radiation going toward sensible heating than the WET or DUNE sites, though the latent and sensible heat flux was partitioned about evenly over the diurnal cycle. Moreover, the greatest variability in the ground heat flux was noted at the DUNE site, with the least variability at the wet valley. With approximately the same amount of net radiation and precipitation measured at all three locations, the differences observed are chiefly due to the varying contributions from subsurface water and the resulting heterogeneity of the site soil and vegetative characteristics.

The Noah LSM was forced using meteorological data from EBBR stations located at each site to assess the

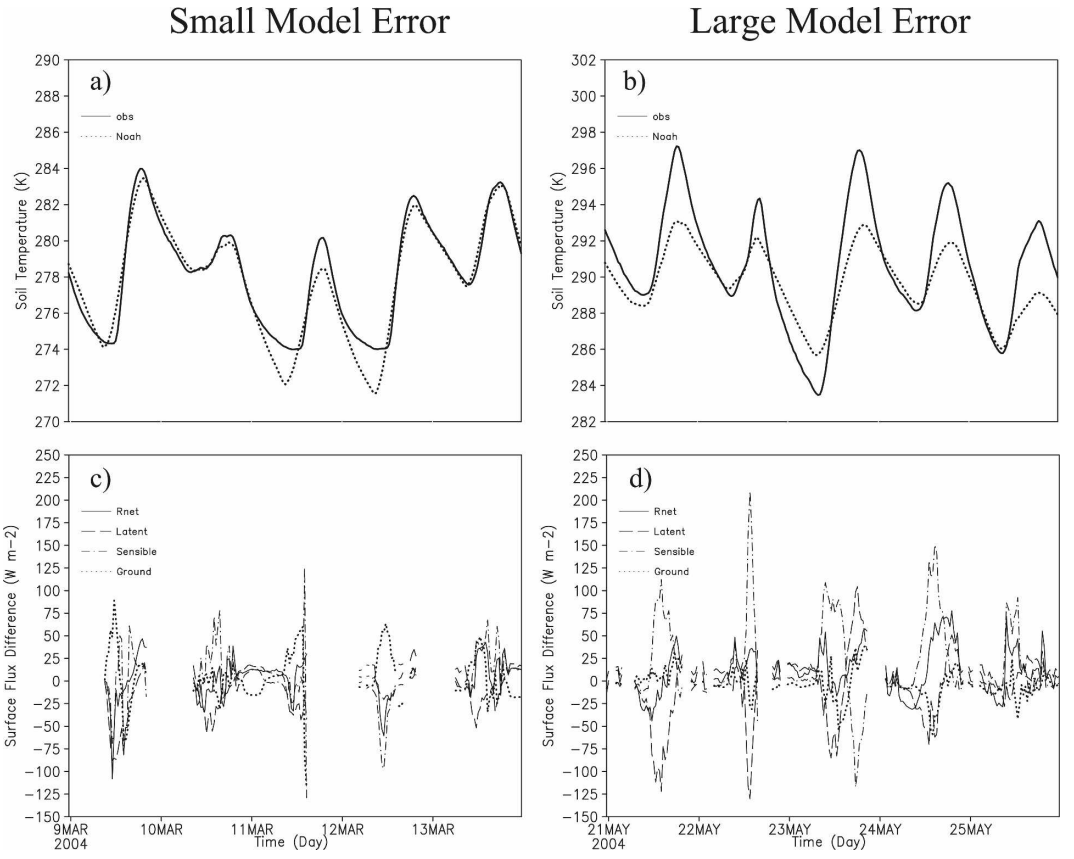


FIG. 11. DUNE 10-cm soil temperature for a case with (a) a small difference and (b) a large temperature difference. (c), (d) The surface flux estimate differences corresponding to (a), (b).

diurnal and annual surface fluxes at these locations. To assess the model's predictive capability for three Sand Hills' locations, evaluation was performed against observations measured at three EBBR meteorological sites and independently verified with an HPRCC AWDN meteorological platform for 2004. Statistical evaluation of the model output revealed that overall, the Noah LSM performed reasonably well in reproducing the surface fluxes at both the DRY and DUNE locations, but exhibited difficulty with the WET location. Errors in net radiation at all three sites were generally within 20% of the mean daily observed value, and were the result of discrepancies in the estimation technique used to compute the incoming longwave radiation for input into the Noah LSM. It was determined that the greatest model error occurred late in the warm season at the WET and DRY valley sites resulting in a positive bias in H for both model simulations. According to annual RMSE values, errors in latent and sensible heat flux at the WET valley were almost twice those of the DRY (and 4 times greater than the DUNE location) site. These errors are chiefly attributed to the lack of a source of subsurface water within the model and resulted in artificially high soil temperatures. The modeled root zone soil moisture is underestimated, particularly during summer when demand for soil water is high and precipitation is low, resulting in less model ET relative to the observations. It was shown that during times of recharge at the DRY valley in the spring and early fall, observed soil water contents increased, but this was not reflected in the model simulation. This created a significant soil moisture deficit by early summer in the Noah LSM, and resulted in underestimates of LE throughout the warm season. This extends the analysis of Evans et al. (2005), who concluded that a version of the Noah LSM coupled to a regional climate model also underestimated ET (LE) and resulted in a positive bias of *H*. In addition, the ground heat flux exhibited a positive bias for all model runs, though correcting for the difference between the modeled surface and observed 10-cm flux estimates indicated a much smaller error.

Further examination of shorter time periods to evaluate the Noah LSM model at high temporal frequency yielded results similar to those over the annual cycle in terms of model error. A comparison of shorter time

periods exhibited the models' inability to capture the diurnal magnitude of $H$ and LE during the late summer. In early August, when the greatest impact of subsurface water is realized due to the lack of precipitation as a recharging agent, the largest overestimation of $H$ and underestimation of LE at each of the valley sites is noted. These large errors (the underestimation of LE in particular) were not noted earlier in the year, indicating that the model soil moisture is significantly underestimated during the late warm season, especially at the WET site, and is not subject to the recharging of the root zone that occurs at the site due to the upward vertical gradient of soil moisture.

When coupled to weather prediction models, land surface schemes provide a lower boundary condition, usually the soil temperature, moisture, and surface fluxes to the parent atmospheric model. Over short spatial and temporal scales, on the order of the lifetime of a thunderstorm for example, correct estimation within the model of the surface fluxes can be extremely important to the development and maintenance of severe convective storms. Erroneous surface flux estimates provided to the atmospheric model can result in spurious convective development, for example when sensible heat flux is too large (increased buoyancy), or increased precipitation when latent heat flux is too large (increased contribution of atmospheric water vapor). Thus, as pointed out this in this study, the influence of a source of subsurface water on local soil moisture appears to hold a strong control on the behavior of surface fluxes over both short and long time scales. In addition, for long time scales of model integration, neglecting this influence can lead to significant errors in surface flux estimations even at very short subtime scales. Future work will examine the addition of a time-varying water table within the lowest layer of the Noah LSM to assess its influence on regional evapotranspiration and the resulting partitioning of the radiation budget.

*Acknowledgments.* This project was part of the Sand Hills Biocomplexity Project supported by the National Science Foundation (BE03-22076). We thank the Research Computing Facility at the University of Nebraska—Lincoln for supercomputer support. We also want to thank T. Arkebauer and D. Billesbach for providing us with the EBBR observed data. The comments and suggestions from three anonymous reviewers strengthened the final version of this manuscript.

## REFERENCES

Adegoke, J. O., R. A. Pielke, J. Eastman, R. Mahmood, and K. G. Hubbard, 2003: Impact of irrigation on midsummer surface fluxes and temperature under dry synoptic conditions: A regional atmospheric model study of the U.S. High Plains. *Mon. Wea. Rev.,* **131,** 556–564.

Allen, R. G., L. Pereira, D. Raes, and M. Smith, 1998: Crop evapotranspiration—Guidelines for computing crop water requirements. FAO irrigation and drainage Paper 56, UN-FAO, Rome, Italy, 297 pp.

Anthes, R. A., 1984: Enhancement of convective precipitation variations in vegetative covering in semiarid regions. *J. Climate Appl. Meteor.,* **23,** 541–554.

Bleed, A., and C. Flowerday, Eds., 1998: *An Atlas of the Sand Hills*. Resource Atlas, No. 5a, Conservation and Survey Division, University of Nebraska, 67–92.

Chen, F., and J. Dudhia, 2001a: Coupling an advanced land surface–hydrology model with the Penn State–NCAR MM5 modeling system. Part I: Model implementation and sensitivity. *Mon. Wea. Rev.,* **129,** 569–585.

——, and ——, 2001b: Coupling an advanced land surface–hydrology model with the Penn State–NCAR MM5 modeling system. Part II: Preliminary model validation. *Mon. Wea. Rev.,* **129,** 587–604.

——, and Coauthors, 1996: Modeling of land surface evaporation by four schemes and comparison with FIFE observations. *J. Geophys. Res.,* **101** (D3), 7251–7266.

Chen, X., and Q. Hu, 2004: Groundwater influences on soil moisture and surface evaporation. *J. Hydrol.,* **297,** 285–300.

Cosby, B. J., G. M. Hornberger, R. B. Clapp, and T. R. Ginn, 1984: A statistical exploration of the relationships of soil moisture characteristics to the physical properties of soils. *Water Resour. Res.,* **20,** 682–690.

Ek, M. B., K. E. Mitchell, Y. Lin, E. Rogers, P. Grunmann, V. Koren, G. Gayno, and J. D. Tarpley, 2003: Implementation of Noah land surface model advances in the National Centers for Environmental Prediction operational mesoscale Eta model. *J. Geophys. Res.,* **108,** 8851, doi:10.1029/2002JD003296.

Evans, J. P., R. J. Oglesby, and W. M. Lapenta, 2005: Time series analysis of regional model climate performance. *J. Geophys. Res.,* **110,** D04104, doi:10.1029/2004JD005046.

Findell, K. L., and E. A. B. Eltahir, 1997: An analysis of the soil moisture-rainfall feedback, based on direct observations from Illinois. *Water Resour. Res.,* **33** (4), 725–735.

Gosselin, D. C., S. Drda, F. E. Harvey, and J. Goeke, 1999: Hydrologic setting of two interdunal valleys in the central Sand Hills of Nebraska. *Ground Water,* **37,** 924–933.

——, V. Sridhar, F. E. Harvey, and J. Goeke, 2006: Hydrological effects and groundwater fluctuations in interdunal environments in the Nebraska Sand Hills. *Gr. Plains Res.,* **16,** 17–28.

Gutman, G., and A. Ignatov, 1998: The derivation of green vegetation fraction from NOAA/AVHRR data for use in numerical weather prediction models. *Int. J. Remote Sens.,* **19,** 1533–1543.

Hogue, T. S., L. Bastidas, H. Gupta, S. Sorooshian, K. Mitchell, and W. Emmerich, 2005: Evaluation and transferability of the Noah land surface model in semiarid environments. *J. Hydrometeor.,* **6,** 68–84.

Hubbard, K. G., 1992: Climate factors that limit daily evapotranspiration in sorghum. *Climate Res.,* **2,** 73–80.

——, N. J. Rosenberg, and D. C. Nielsen, 1983: Automated weather data network for agriculture. *J. Water Resour. Plann. Manage.,* **109,** 213–222.

Juang, J.-Y., A. Porporato, P. C. Stoy, M. S. Siqueira, A. C. Oishi,

M. Detto, H.-S. Kim, and G. G. Katul, 2007: Hydrologic and atmospheric controls on initiation of convective precipitation events. *Water Resour. Res.,* **43,** W03421, doi:10.1029/2006WR004954.

Mahmood, R., and K. G. Hubbard, 2004: An analysis of simulated long-term soil moisture data for three land uses under contrasting hydroclimatic conditions in the Northern Great Plains. *J. Hydrometeor.,* **5,** 160–179.

Mahrt, L., and M. Ek, 1984: The influence of atmospheric stability on potential evaporation. *J. Climate Appl. Meteor.,* **23,** 222–234.

——, and H. L. Pan, 1984: A two-layer model of soil hydrology. *Bound.-Layer Meteor.,* **29,** 1–20.

Maxwell, R. M., and N. L. Miller, 2005: Development of a coupled land surface and groundwater model. *J. Hydrometeor.,* **6,** 233–247.

McCumber, M. C., and R. A. Pielke, 1981: Simulation of the effects of surface fluxes of heat and moisture in a mesoscale numerical model. *J. Geophys. Res.,* **86,** 9929–9938.

Mitchell, K., and Coauthors, cited 2001: The community NOAH land-surface model user's guide version 2.3. [Available online at ftp://ftp.emc.ncep.noaa.gov/mmb/gcp/ldas/noahlsm/ver_2.7.1/Noah_LSM_USERGUIDE_2.7.1.htm.]

Mohr, K. I., J. S. Famiglietti, A. Boone, and P. J. Starks, 2000: Modeling soil moisture and surface flux variability with an untuned land surface scheme: A case study from the Southern Great Plains 1997 Hydrology Experiment. *J. Hydrometeor.,* **1,** 154–169.

Monteith, J. L., 1963: Dew: Facts and fallacies. *The Water Relations of Plants,* A. J. Rutter and F. H. Whitehead, Eds., Blackwell Scientific Publications, 37–56.

Nash, J. E., and J. V. Sutcliffe, 1970: River flow forecasting through conceptual models, Part I—A discussion of principles. *J. Hydrol.,* **10,** 282–290.

Ronda, R. J., B. J. J. M. van den Hurk, and A. A. M. Holtslag, 2002: Spatial heterogeneity of the soil moisture content and its impact on surface flux densities and near-surface meteorology. *J. Hydrometeor.,* **3,** 556–570.

Skamarock, W. C., J. B. Klemp, J. Dudhia, D. O. Gill, D. M. Barker, W. Wang, and J. G. Powers, 2005: A description of the Advanced Research WRF version 2. NCAR Tech Note NCAR/TN-468+STR, 88 pp. [Available from UCAR Communications, P. O. Box 3000, Boulder, CO 80307.]

Small, E. E., and S. A. Kurc, 2003: Tight coupling between soil moisture and the surface radiation budget in semiarid environments: Implications for land–atmosphere interactions. *Water Resour. Res.,* **39,** 1278, doi:10.1029/2002WR001297.

Sridhar, V., and R. L. Elliott, 2002: On the development of a simple downwelling longwave radiation scheme. *Agric. For. Meteor.,* **112,** 237–243.

——, ——, F. Chen, and J. A. Brotzge, 2002: Validation of the NOAH-OSU land surface model using surface flux measurements in Oklahoma. *J. Geophys. Res.,* **107,** 4418, doi:10.1029/2001JD001306.

——, K. G. Hubbard, and D. A. Wedin, 2006: Assessment of soil moisture dynamics of the Nebraska Sand Hills using long-term measurements and a hydrology model. *J. Irrig. Drain. Eng.,* **132,** 463–473.

Stull, R. B., 1988: *An Introduction to Boundary Layer Meteorology*. Kluwer Academic, 666 pp.

Twine, T. E., C. J. Kucharik, and J. A. Foley, 2004: Effects of land cover change on the energy and water balance of the Mississippi River Basin. *J. Hydrometeor.,* **5,** 640–655.

Wilks, D. S., 1995: *Statistical Methods in the Atmospheric Sciences*. Academic Press, 467 pp.